Optica Applicata, Vol. XXXIV, No. 2, 2004

Opto structural effects of annealing of Nylon 66 fibers

I.M. FOUDA, F.M. EL-SHARKAWY

Physics Department of Science, Mansoura University, Mansoura, Egypt.

Multiple-beam Fizeau fringes are used to study the changes in optical parameters of annealed Nylon 66 fibers. Changes in the refractive indices and birefringence of skin and core have been measured interferometrically. The application was carried out using multiple-beam Fizeau fringes in transmission to determine the principal optical parameters characterizing the skin-core layers. The density of the fibers was measured by a system based on the theory of vibrating strings. The results of density and optical measurement were used to calculate the degree of crystallinity, the form birefringence, the number of monomeric units per unit volume, the harmonic mean polarizability of the dielectric, the harmonic mean specific refractivity and the virtual refractive index. The results also were used to obtain the stress-optical coefficient C_s, the optical configuration parameter Δa, the mean square density fluctuation $<\eta^2>$, the segment anisotropy γ_s, molar refractivity R and the thermal stress σ in different annealing conditions. The results clarify the reorientation, and layer changes occuring due to annealing conditions. The optical orientation function and the angle of orientation are also calculated. Relations between the optical parameters with different thermal effects are discussed.

Keywords: orientation, crystallinity, annealing, Nylon 66, skin-core, interferometry.

1. Introduction

It is known that birefringence Δn_a is one of the most sensitive indicators of the extent of anisotropy of the properties of polymer and therefore, the degree of macromolecular orientation. The coefficient of birefringence Δn_a is often used as a measure of polymer orientation since the value of Δn_a has a relation with the average square deviation of orientation of macromolecules from the isotropic state [1].

The thermal treatment of polymers causes structural and chemical variations, which in turn lead to variations in physical properties. The changes in the optical anisotropy and orientation in polymer fibers by heat treatments can be evaluated interferometrically by the measurement of refractive indices and birefringence of these fibers. These optical properties provide parameters that characterize the structure of the polymer on the molecular level. Annealed and quenched fibers can be investigated by the measurement of the optical anisotropy of these fibers [2]–[10].

Fiber technologists, and in particular those dealing with wet-spinning and melt-spun ascribe considerable importance to so-called “skin-core” structure. In many

fiber types the cross-section is distinctly divided into outer and inner parts called respectively “skin” and “core” having different affinity to dyes. The many possible mechanisms of formation of the skin-core structure are discussed elsewhere [11]–[14].

Recently two or multiple-beam interference were applied to determine the optical parameters of synthetic and natural fibers [15]–[21]. Characterization of these fibers is important for the textile industry and the end use. The density of annealed Nylon 66, measured by a system based on a vibrating string, has been discussed in detail elsewhere [8], [9]. The density results can be used to follow the changes of the degree of crystallinity.

In this work, the optical parameters and results of density measurement, for samples of Nylon 66 under different annealing conditions, are used to calculate some optical structural parameters for the skin-core layers and the mean values considering the fiber as a single medium.

2. Theoretical considerations

2.1. Interferometric measurements of the optical parameters

Multiple beam Fizeau fringes [19], [20] in transmission were used for the determination of the basic optical parameters of Nylon 66 fibers for skin-core layers. The experimental values of the refractive indices and polarizabilities were used to calculate

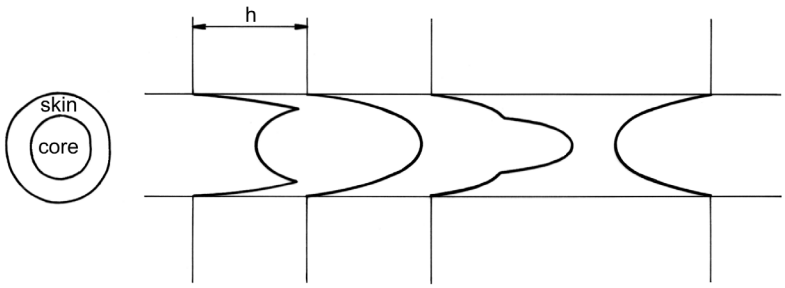

Fig. 1. Schematic diagram for skin-core structure fringes shift in the case of skin-core structure for different values of the refractive index of the immersed liquid n_L.

the number of molecules per unit volume. Figure 1 shows schematic diagram for skin-core structure fringes.

2.2. Mean refractive index n_a

The obtained mean refractive index n_a of Nylon 66 fibers, having core surrounded by a skin layer is reported in Tab. 1.

2.3. Mean polarizability of monomer unit

The polarizability of a monomer unit like the polarizability of a simple organic molecule usually varies in different directions. As the refractive index of a polymer

T a b l e 1a. Skin values parameters.

Annealing temperature [°C]	$n_s^{\parallel}$	$n_s^{\perp}$	n_v	n_{iso}	$N_{(1)} \times 10^{22}$	$\frac{F_\theta}{F_\Delta}$	$\frac{F_\theta - F_\Delta}{F_\theta}$
Unannealed	1.5815	1.5035	1.5270	1.5153	30.5	0.944	–0.059
90	1.5909	1.5203	1.5418	1.5333	30.3	0.920	–0.087
110	1.5898	1.5190	1.5406	1.5093	31.4	0.922	–0.084
130	1.5896	1.5190	1.5405	1.5394	29.9	0.922	–0.084
150	1.5923	1.5178	1.5404	1.5140	31.2	0.921	–0.085
160	1.5905	1.5220	1.5429	1.4913	32.5	0.920	–0.088
170	1.5937	1.5246	1.5457	1.5200	31.1	0.914	–0.094
180	1.5937	1.5284	1.5485	1.5168	31.4	0.910	–0.098

T a b l e 1b. Core values parameters.

Annealing temperature [°C]	$n_c^{\parallel}$	$n_c^{\perp}$	n_v	n_{iso}	$N_{(1)} \times 10^{22}$	$\frac{F_\theta}{F_\Delta}$	$\frac{F_\theta - F_\Delta}{F_\theta}$
Unannealed	1.5843	1.4969	1.5229	1.5118	30.5	0.956	–0.046
90	1.5937	1.5137	1.5377	1.5298	30.3	0.924	–0.082
110	1.5941	1.5159	1.5395	1.5086	31.4	0.921	–0.085
130	1.5943	1.5170	1.5403	1.5395	29.9	0.920	–0.086
150	1.5949	1.5159	1.5397	1.5135	31.2	0.920	–0.086
160	1.5908	1.5188	1.5407	1.4895	32.5	0.921	–0.085
170	1.5974	1.5224	1.5451	1.5197	31.1	0.912	–0.095
180	1.6022	1.5246	1.5481	1.5169	31.4	0.906	–0.103

T a b l e 1c. Mean values parameters.

Annealing temperature [°C]	$n_a^{\parallel}$	$n_a^{\perp}$	n_v	n_{iso}	$N_{(1)} \times 10^{22}$	$\frac{F_\theta}{F_\Delta}$	$\frac{F_\theta - F_\Delta}{F_\theta}$
Unannealed	1.5830	1.5000	1.5248	1.5134	30.5	0.945	–0.057
90	1.5924	1.5168	1.5397	1.5315	30.3	0.922	–0.085
110	1.5921	1.5173	1.5400	1.5089	31.4	0.922	–0.084
130	1.5921	1.5179	1.5404	1.5395	29.9	0.921	–0.085
150	1.5937	1.5168	1.5400	1.5137	31.2	0.921	–0.085
160	1.5907	1.5203	1.5418	1.4903	32.5	0.920	–0.086
170	1.5956	1.5235	1.5454	1.5198	31.1	0.914	–0.094
180	1.5982	1.5264	1.5483	1.5169	31.4	0.908	–0.100

depends on the total polarizability of the molecules, this leads to the Lorentz–Lorenz equations [22]

$$\frac{\bar{n}^2 - 1}{\bar{n}^2 + 2} = \frac{N_{(1)}\bar{\alpha}}{3\psi} \tag{1}$$

where $\bar{n}$ is the average refractive index, ψ is the permittivity of free space equal to 8.85×10^{-12} F/m ($m^{-3}K^{-1}S^4A^2$) and $\bar{\alpha}$ the mean polarizability of a monomer unit.

For a bulk polymer of density ρ and monomer unit molecular weight M, the number of monomer units per unit volume $N_{(1)} = N_A\rho/M$ (where N_A is Avogadro's number 6.02×10^{23} and for Nylon 66 $M = 226$ [22]), which is also equal the number of carries of the dipole moment. Also from analogous equations using the refractive indices we can obtain $\varepsilon^{\|}$, $\varepsilon^{\perp}$ and ε_v.

De Vries [23] developed a theory on the basis of internal field with the aid of classical electromagnetic theory, in which he generalized the Lorentz–Lorenz equation, so for monochromatic light, the well known Lorentz–Lorenz becomes as Eq. (1). The right-hand member of Eq. (1) is proportional to the density ρ [Kg/m^3] of the medium and may also be written as

$$\frac{n^2-1}{n^2+2} = \bar{\varepsilon}\rho \tag{2}$$

where $\bar{\varepsilon}$ [m^3/Kg] is called the specific refractivity of the isotropic dielectric. Also, from analogous equations we can obtain $\alpha^{\|}$, $\alpha^{\perp}$ and α_v.

De Vries defined the invariant refractive index as well, which he called the virtual refractive index n_v,

$$n_v = \sqrt{1+\frac{3\left(n_{\|}^2-1\right)\left(n_{\perp}^2-1\right)}{\left(n_{\perp}^2-1\right)+2\left(n_{\|}^2-1\right)}} \tag{3}$$

where the virtual refractive index n_v replaces the well-known isotropic refractive index, calculated by the equation used in our previous publication [24].

The harmonic mean polarizability of the dielectric α_v can be given by the following equation:

$$\alpha_v = \frac{3\psi}{N_{(1)}}\frac{n_v^2-1}{n_v^2+2}. \tag{4}$$

Likewise, for the harmonic mean specific refractivity, we have

$$\varepsilon_v = \rho^{-1}\frac{n_v^2-1}{n_v^2+2}. \tag{5}$$

In a recent approach to the continuum theory of birefringence of oriented polymer [23], orientation function F_θ was found. Also, using HERMANS and PLATZEK [25] and KRATKY [26] equations, one can derive the following equations:

$$F_\theta = (1 + a)F_\Delta - aF_\Delta^2,$$

$$(1 + a) = \frac{2 n_1^2 n_2^2}{n_v^3 (n_1 + n_2)} \tag{6}$$

where n_1, n_2 are the refractive indices of fully oriented fiber, using monochromatic light vibrating parallel and perpendicular to the fiber axis. From Eq. (6) the constant a was calculated and found to be equal to 0.5.

The evaluation of orientation function for partially oriented aggregate $\langle P_2(\theta)\rangle$ is defined by WARD [27] by the following equation, which is the same function F_Δ named by HERMANS [28]

$$F_\Delta = \langle P_2(\theta)\rangle = \frac{\Delta n}{\Delta n_{\max}}. \tag{7}$$

CUNNINGHAM *et al*. [29] derived a relation between the optical orientation function $\langle P_2(\theta)\rangle$ and the polarizability as follows:

$$\frac{\Phi^{\parallel} - \Phi^{\perp}}{\Phi^{\parallel} + 2\Phi^{\perp}} = \frac{\Delta\alpha}{3\alpha_o}\langle P_2(\theta)\rangle \tag{8}$$

where $\Phi^{\parallel} = \left(n_{\parallel}^2 - n_{\perp}^2\right)\Big/\left(n_{\parallel}^2 + 2n_{\perp}^2\right)$ and analogous equation for $\Phi^{\perp}$ and $(\Delta\alpha/3\alpha_o)$ is found to be $\cong 0.05$ for Nylon 66, which is in agreement with the previously published results [30].

2.4. Crystallinity equation

The degree of crystallinity χ understood as the volume fraction of crystalline material was determined by the relation [31]

$$\chi = \frac{\rho - \rho_a}{\rho_c - \rho_a} \tag{9}$$

where ρ_c and ρ_a are the densities of the crystalline and non-crystalline regions, ρ is the experimental measured value of density, with $\rho_c = 1.236\times10^3$ kg/m^3 [32] and $\rho_a = 1.12\times10^3$ kg/m^3 [33]. The results of ρ and χ measurements for Nylon 66 fibers are shown in Tab. 2.

T a b l e 2a. Skin values parameters.

Annealing temperature [°C]	ρ	χ [%]	Δn_f	$\langle \eta^2 \rangle$	$\sigma \times 10^{12}$	$\Delta a \times 10^{-32}$	R	R'
Unannealed	1.1450	21.55	–0.0054	0.0023	0.5640	0.0328	62.17	9.920
90	1.1376	15.17	–0.0136	0.0017	0.5604	0.0296	63.82	10.32
110	1.1803	51.98	–0.0090	0.0034	0.5814	0.0286	61.40	10.28
130	1.1247	4.052	–0.0149	0.0005	0.5540	0.0299	64.43	10.28
150	1.1712	44.14	–0.0062	0.0033	0.5769	0.0303	61.94	10.30
160	1.2210	87.07	–0.0071	0.0015	0.6015	0.0267	59.52	10.34
170	1.1688	42.07	–0.0119	0.0033	0.5757	0.0281	62.44	10.43
180	1.1794	51.21	–0.0146	0.0034	0.5810	0.0263	62.06	10.49

T a b l e 2b. Core values parameters.

Annealing temperature [°C]	ρ	χ [%]	Δn_f	$\langle \eta^2 \rangle$	$\sigma \times 10^{12}$	$\Delta a \times 10^{-32}$	R	R'
Unannealed	1.1450	21.55	0.0040	0.0023	0.5640	0.0368	61.99	9.862
90	1.1376	15.17	–0.0042	0.0017	0.5604	0.0335	63.64	10.26
110	1.1803	51.98	–0.0016	0.0034	0.5814	0.0316	61.45	10.30
130	1.1247	4.052	–0.0082	0.0005	0.5540	0.0327	64.56	10.32
150	1.1712	44.14	–0.0017	0.0033	0.5769	0.0321	61.97	10.31
160	1.2210	87.07	–0.0036	0.0015	0.6015	0.0281	59.39	10.30
170	1.1688	42.07	–0.0060	0.0033	0.5757	0.0305	62.51	10.45
180	1.1794	51.21	–0.0023	0.0034	0.5810	0.0312	62.27	10.56

T a b l e 2c. Mean values parameters.

Annealing temperature [°C]	ρ	χ [%]	Δn_f	$\langle \eta^2 \rangle$	$\sigma \times 10^{12}$	$\Delta a \times 10^{-32}$	R	R'
Unannealed	1.1450	21.55	–0.0004	0.0023	0.5640	0.0349	62.07	9.890
90	1.1376	15.17	–0.0086	0.0017	0.5604	0.0317	63.73	10.29
110	1.1803	51.98	–0.0050	0.0034	0.5814	0.0302	61.43	10.29
130	1.1247	4.052	–0.0113	0.0005	0.5540	0.0314	64.50	10.30
150	1.1712	44.14	–0.0038	0.0033	0.5769	0.0313	61.95	10.31
160	1.2210	87.07	–0.0052	0.0015	0.6015	0.0275	59.45	10.32
170	1.1688	42.07	–0.0089	0.0033	0.5757	0.0293	62.48	10.44
180	1.1794	51.21	–0.0081	0.0034	0.5810	0.0289	62.17	10.53

2.5. Calculation of the isotropic refractive index

The Lorentz–Lorenz equation is used to relate polarizabilities and refractive indices by the following equation [29]:

$$\frac{n_{\mathrm{iso}}^2 - 1}{n_{\mathrm{iso}}^2 + 2} = \frac{\rho_i}{3\rho}\left[\frac{n_{\parallel}^2 - 1}{n_{\parallel}^2 + 2} + 2\,\frac{n_{\perp}^2 - 1}{n_{\perp}^2 + 2}\right] \tag{10}$$

where ρ and ρ_i are the densities of the measured and of the isotropic polymer tested, respectively. The obtained values of $n_a^{\parallel}$, $n_a^{\perp}$ and ρ are used with Eq. (10) to determine the isotropic refractive index values for annealed Nylon 66 fibers, for the mean values where $\rho_i = \rho_a = 1.12 \times 10^3$ kg/m^3.

2.6. Evaluation of the form birefringence

The total birefringence for a fiber is the sum of three components

$$\Delta n = \chi_c \Delta n_c + (1 - \chi_c)\Delta n_a + \Delta n_f, \tag{11}$$

where Δn_c is the birefringence per unit volume of crystalline material, Δn_a – the birefringence per unit volume of amorphous material, Δn_f – the form birefringence, and χ_c – the volume fraction of crystalline regions [34].

2.7. Mean square density fluctuation $\langle \eta^2 \rangle$

For a two-phase structure consisting of amorphous and crystalline regions with densities ρ_a and ρ_c, respectively, the mean square density fluctuation $\langle \eta^2 \rangle$, can be calculated from the following equation [35]

$$\langle \eta^2 \rangle = (\rho_c - \rho_a)^2 \chi (1 - \chi). \tag{12}$$

The values of Δn_f and $\langle \eta^2 \rangle$ for Nylon 66 fibers are given in Tab. 2.

2.8. Average optical orientation [36]

The overall orientation F_{av} was calculated from birefringence measurements of individual fibers. The average orientation F_{av} was calculated from the following equation:

$$F_{av} = \frac{2\Delta n}{\Delta n_c^o + \Delta n_a^o} \tag{13}$$

where the denominator is composed of the intrinsic birefringence of crystals and the ideal amorphous birefringence $\Delta n_c^o = 0.074$, $\Delta n_a^o = 0.086$, $\Delta n_{\max}^o = 0.082$.

2.9. Stress-optical coefficient

The value of the stress-optical coefficient C_s depends on the chemical structure of the polymer. Also the value of this coefficient depends solely on the mean refractive index and the optical anisotropy of the random link, as seen from the following equation [37]

$$C_s = \frac{2\pi}{45KT} \frac{\left(\bar{n}^2 + 2\right)^2}{\bar{n}} (\alpha_1 - \alpha_2) \tag{14}$$

where α_1 and α_2 are the polarizabilities of monomer units along and across the axis of such units and K is the Boltzmann constant.

From the above equation it can be seen that birefringence in elastomers is proportional to the stress which occurred.

2.10. Segment anisotropy [38]

As the segment anisotropy γ_s is related to the stress optical coefficient this leads to the following equation:

$$C_s = \frac{\gamma_s}{90\psi KT}\frac{\left(\bar{n}^2+2\right)^2}{\bar{n}}. \tag{15}$$

So, we can determine γ_s.

2.11. Determination of thermal stress

A transformation of initially crystalline and amorphous fibers by thermal treatment to introduce structural changes is also known, as polymer chains align in the direction of an applied thermal stress due to mobility of the molecules. The average chain orientation of both amorphous and crystalline regions in the network, were measured by birefringence in the present work, so we can obtain the deformation thermal stress from the following equation:

$$C_s = \frac{\Delta n}{\sigma}. \tag{16}$$

2.12. Optical configuration parameter [37]

The optical configuration parameter Δa is related to the stress-optical coefficient C_s by the following equation:

$$\Delta a = \frac{(45KTC_s/2\pi)n}{\left(\bar{n}^2+2\right)^2} \tag{17}$$

where $\Delta a = \alpha_1 - \alpha_2$ from Eq (17). Values of Δa at different values of n and C_s are summarized in Tab. 2.

2.13. Molar refractivity [39]

The polarizability of a molecule is related to its refractive index by the Lorentz –Lorenz relation

$$\frac{\bar{n}^2 - 1}{\bar{n}^2 + 2}\frac{M}{\rho} = R \tag{18}$$

where ρ is the density, and R is the molecular or molar refractivity. The value M is understood as the repeat unit of the molecule.

T a b l e 3a. Skin values parameters.

Annealing temperature [°C]	$P_s^{\parallel}$	$P_s^{\perp}$	$N_{(2)}$	$\alpha_s^{\parallel}\times10^{-32}$	$\alpha_s^{\perp}\times10^{-32}$	$\bar{\alpha}\times10^{-32}$	$\varepsilon_s^{\parallel}$	$\varepsilon_s^{\perp}$	$\bar{\varepsilon}$
Unannealed	0.0796	0.0706	22.67	0.2904	0.2576	0.2742	0.2913	0.2584	0.2751
90	0.0806	0.0726	22.79	0.2961	0.2665	0.2815	0.2970	0.2674	0.2824
110	0.0805	0.0724	22.78	0.2849	0.2564	0.2708	0.2858	0.2572	0.2717
130	0.0805	0.0724	22.78	0.2989	0.2690	0.2842	0.2999	0.2699	0.2851
150	0.0808	0.0723	22.78	0.2881	0.2578	0.2732	0.2891	0.2587	0.2741
160	0.0809	0.0728	22.80	0.2757	0.2490	0.2625	0.2766	0.2498	0.2634
170	0.0809	0.0731	22.82	0.2893	0.2612	0.2754	0.2902	0.2620	0.2763
180	0.0799	0.0735	22.84	0.2867	0.2604	0.2737	0.2876	0.2613	0.2746

T a b l e 3b. Core values parameters.

Annealing temperature [°C]	$P_s^{\parallel}$	$P_s^{\perp}$	$N_{(2)}$	$\alpha_s^{\parallel}\times10^{-32}$	$\alpha_s^{\perp}\times10^{-32}$	$\bar{\alpha}\times10^{-32}$	$\varepsilon_s^{\parallel}$	$\varepsilon_s^{\perp}$	$\bar{\varepsilon}$
Unannealed	0.0799	0.0698	22.65	0.2915	0.2547	0.2734	0.2924	0.2555	0.2743
90	0.0809	0.0718	22.77	0.2972	0.2637	0.2807	0.2982	0.2645	0.2816
110	0.0810	0.0721	22.78	0.2866	0.2551	0.2711	0.2875	0.2559	0.2719
130	0.0810	0.0722	22.79	0.3009	0.2682	0.2848	0.3018	0.2690	0.2857
150	0.0811	0.0721	22.79	0.2892	0.2570	0.2734	0.2901	0.2579	0.2742
160	0.0806	0.0724	22.78	0.2758	0.2477	0.2620	0.2767	0.2485	0.2628
170	0.0814	0.0728	22.83	0.2908	0.2603	0.2757	0.2917	0.2611	0.2766
180	0.0819	0.0731	22.87	0.2900	0.2589	0.2747	0.2909	0.2597	0.2755

T a b l e 3c. Mean values parameters.

Annealing temperature [°C]	$P_s^{\parallel}$	$P_s^{\perp}$	$N_{(2)}$	$\alpha_s^{\parallel}\times10^{-32}$	$\alpha_s^{\perp}\times10^{-32}$	$\bar{\alpha}\times10^{-32}$	$\varepsilon_s^{\parallel}$	$\varepsilon_s^{\perp}$	$\bar{\varepsilon}$
Unannealed	0.0798	0.0702	22.66	0.2910	0.2561	0.2738	0.2919	0.2569	0.2747
90	0.0808	0.0722	22.78	0.2967	0.2650	0.2811	0.2976	0.2659	0.2820
110	0.0808	0.0722	22.78	0.2858	0.2556	0.2710	0.2868	0.2565	0.2718
130	0.0808	0.0723	22.78	0.3000	0.2685	0.2845	0.3009	0.2694	0.2854
150	0.0809	0.0722	22.79	0.2887	0.2574	0.2733	0.2896	0.2582	0.2742
160	0.0806	0.0726	22.79	0.2758	0.2483	0.2622	0.2767	0.2491	0.2631
170	0.0812	0.0730	22.83	0.2900	0.2608	0.2756	0.2910	0.2616	0.2765
180	0.0814	0.0733	22.86	0.2885	0.2596	0.2742	0.2894	0.2604	0.2751

2.14. Calculation of the surface reflectivity

The surface reflectivity of polymer for light at normal incidence can be estimated from Fresnel's equation [39] and knowledge of the mean refractive index $\bar{n}$. Thus the percentage reflection R' (for two surfaces in air) is given by

$$R' = \left(\frac{\bar{n} - 1}{\bar{n} + 2}\right)^2 \times 100. \tag{19}$$

2.15. Determination of the skin, core and mean polarizability per unit volume of Nylon 66 fibers

The values for skin and core polarizabilities per unit volume $P_s^{\parallel}$, $P_s^{\perp}$, $P_c^{\parallel}$, and $P_c^{\perp}$ as well as the mean polarizabilities per unit volume $P_a^{\parallel}$ and $P_a^{\perp}$ were calculated using the equation from our previous publication [9].

The calculated skin and core refractive indices along with the mean refractive indices of Nylon 66 fibers for plane polarized light, vibrating parallel and perpendicularly to the fiber axis, served the purpose.

The variation of $P_s^{\parallel}$, $P_c^{\parallel}$, $P_a^{\parallel}$, $P_s^{\perp}$, $P_c^{\perp}$, and $P_a^{\perp}$ with different annealing temperature (90–180 ± 1 °C) at constant annealing time of 6 hrs for Nylon 66 fiber are shown in Tab. 3.

2.16. Determination of the number of molecules per unit volume

The birefringence of the sample for the beams polarized respectively along the longitudinal and transverse axes is linked with the difference in the mean polarizabilites of the macromolecules for the same direction $(P_{\parallel} - P_{\perp})$ by the following relation [41]:

$$\Delta n = \frac{2\pi N_2}{\bar{n}}\left(\frac{\bar{n}^2 + 2}{3}\right)^2 (\bar{P}_{\parallel} - \bar{P}_{\perp}) \tag{20}$$

where N_2 is the number of molecules per unit volume.

So, by applying multiple-beam Fizeau fringes analogous equations as previously mentioned (see Eqs. (3)–(20)) could be used to obtain the structural parameters for the skin and core layers from results of their optical measurements. Also the same mean structural parameters can be obtained when we consider the fiber containing one layer (single medium).

3. Experimental procedure and results

3.1. Annealing process

For the annealing conditions used, the Nylon 66 fibers were distributed in a cocoon form on glass rods with free ends. They were then heated in an electric oven at different

annealing temperatures (90–180 ± 1 °C) and constant time intervals of 6 hrs, then left to cool in air at room temperature.

3.2. Measurements of transverse sectional area for fibers

Measurements of transverse sectional area for Nylon 66 fibers showed that the cross -section of the Nylon 66 fibers observed by high power optical microscopy is perfectly circular. The fiber had a diameter of 19 μm.

3.3. Interferometric measurements of the optical parameters (multiple-beam Fizeau fringes in transmission for determining the skin, core and mean refractive indices and the birefringence of Nylon 66 fibers)

Figure 2 shows the optical system which was used to produce multiple-beam Fizeau fringes in transmission. A parallel beam of plane polarized monochromatic light of wavelength λ is used to illuminate a wedge interferometer placed on a microscope stage. The fiber is immersed in a liquid and its orientation is perpendicular to the edge of the wedge. Straight line fringes parallel to the edge of the wedge are formed in the liquid region. The amount, shape and direction of fringe shift crossing the fiber depends on the refractive index of liquid n_L, the relative refractive indices of the skin and core and on the wavelength and the state of polarization of monochromatic light used. Mathematical expressions were derived by NICKLAWY and FOUDA [20] for the shape of multiple-beam Fizeau fringes crossing multiplayer fibers of rgular transverse sections immersed in a silvered liquid wedge.

Multiple-beam Fizeau fringes in transmission were used for determining the optical parameters of the skin, core and mean refractive indices, namely $n_s^{\parallel}$, $n_s^{\perp}$, $n_c^{\parallel}$, $n_c^{\perp}$, $n_a^{\parallel}$ and $n_a^{\perp}$. The skin, core and mean birefringence, Δn_s, Δn_c, and Δn_a, were also calculated. The values were determined for several samples of Nylon 66 fibers. Throughout this experiment, the green wavelength of a mercury lamp of 546.1 nm was used.

Figure 3 is a microinterferogram of multiple-beam Fizeau fringes in transmission of an unannealed Nylon 66 fibers, in parallel and perpendicular direction, respectively.

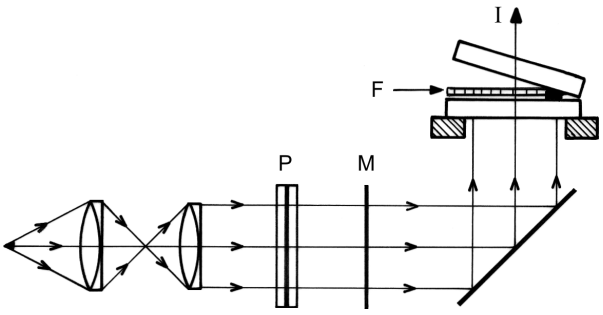

Fig. 2. Setup for producing multiple-beam Fizeau fringes in transmission (P – polarizer, M – monochromatic filter, F – fibre immersed in silvered liquid wedge interferometer, I – camera).

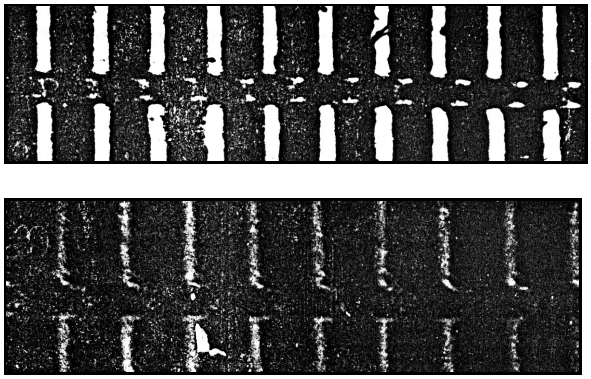

Fig. 3. Microinterferogram of multiple-beam Fizeau fringes in transmission of an unannealed Nylon 66 fiber, in parallel and perpendicular directions, respectively, at wavelength $\lambda = 546$ nm.

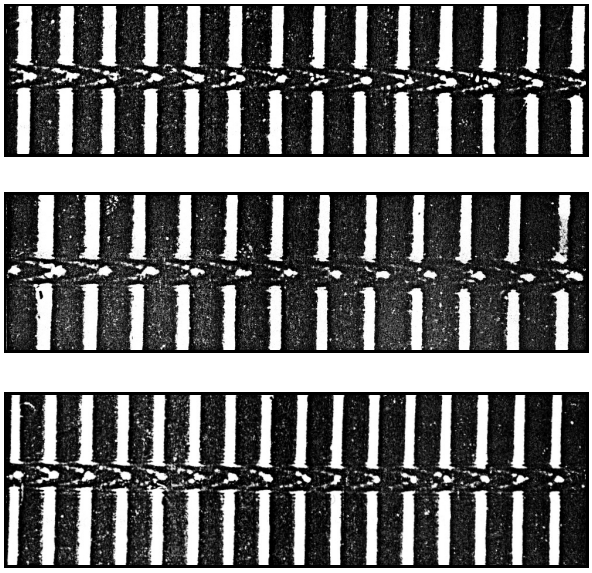

Fig. 4. Microinterferogram of multiple-beam Fizeau fringes in transmission of Nylon 66 fiber annealed for constant time of 6 hrs at different annealing temperatures, in parallel direction at wavelength $\lambda = 546$ nm.

The microinterferograms of multiple-beam Fizeau fringes in transmission of Nylon 66 fiber, shown in Figs. 4 and 5 correspond to fiber annealed for constant time of 6 hrs at different annealing temperatures, in parallel and perpendicular directions, respectively. The refractive indices of the immersion liquid used for parallel and perpendicular component of the fiber were 1.584 at 18 ± 1 °C and 1.529 at 18 ± 1 °C, respectively.

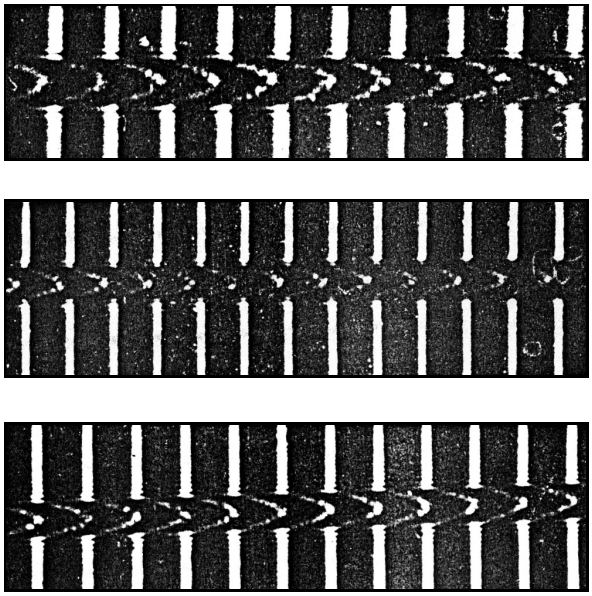

Fig. 5. Microinterferogram of multiple-beam Fizeau fringes in transmission of Nylon 66 fiber annealed for constant time of 6 hrs at different annealing temperatures, in perpendicular direction at wavelength $\lambda = 546$ nm.

The fringe shift of the fiber in Fig. 5 was found to be away from the apex of the interferometer. This indicated that, for perpendicular component, the refractive index of the selected liquid was higher than that of the fiber. It was observed from Figs. 4 and 5 that as annealing temperatures were increased the fringe shift decreased, *i.e.*, the refractive index of the annealed fiber increased with the increase of the annealing temperature.

The values of the fringe shift for the parallel component of both the fiber skin $\mathrm{d}z_s^{\parallel}$ and the fiber core $\mathrm{d}z_c^{\parallel}$ and the interfering spacing h were measured from microinterferograms. The thickness of the skin r_s and the radius of the core r_c were also obtained from the microinterferograms. The radius of the fiber r_f was deduced from both the microinterferograms and from the optical cross-section obtained. Analogous formula was obtained for the other direction $n_s^{\perp}$ and $n_c^{\perp}$. In Fig. 6 the variations of $n_s^{\parallel}$, $n_c^{\parallel}$, $n_a^{\parallel}$, $n_s^{\perp}$, $n_c^{\perp}$, and $n_a^{\perp}$, with the different annealing temperatures for the constant annealing time of 6 hrs are observed.

The refractive indices obtained were used to find values for: Δn_s , Δn_c, and Δn_a, see Fig. 7.

Figure 8 shows the relation between the birefringence Δn_s , Δn_c, Δn_a and the differences of refractive indices: $n_s^{\parallel} - n_{\mathrm{iso}}$, $n_s^{\perp} - n_{\mathrm{iso}}$, $n_s^{\parallel} - n_v$, $n_s^{\perp} - n_v$, $n_c^{\parallel} - n_{\mathrm{iso}}$, $n_c^{\perp} - n_{\mathrm{iso}}$, $n_c^{\parallel} - n_v$, $n_c^{\perp} - n_v$, $n_a^{\parallel} - n_{\mathrm{iso}}$, $n_a^{\perp} - n_{\mathrm{iso}}$, $n_a^{\parallel} - n_v$, $n_a^{\perp} - n_v$. Values presented in Fig. 8, n_v and $\Delta n_{\max}$, are used to predict values of the refractive indices n_1 and n_2

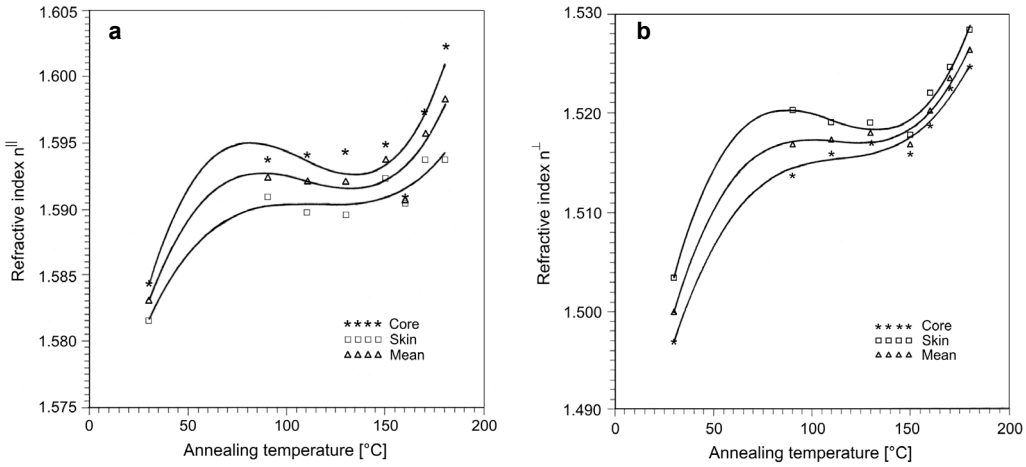

Fig. 6. Variations of $n_s^{\parallel}$, $n_c^{\parallel}$, $n_a^{\parallel}$, (**a**) and $n_s^{\perp}$, $n_c^{\perp}$, $n_a^{\perp}$, (**b**) with the different annealing temperatures for the constant annealing time of 6 hrs.

for fully oriented fibers. These values are found to be 1.575 and 1.494, respectively, at 28 °C. Table 1 gives some experimental results for annealed Nylon 66 fibers, refractive indices, virtual refractive index n_v, isotropic refractive index and the calculated values of the number of monomer units per unit volume N_1. Skin, core layer and mean values of F_θ/F_Δ and $(F_\theta - F_\Delta)/F_\theta$ are found for annealed Nylon 66 fibers, with the results being given in Tab. 1. These values are in fair agreement with similar polymers (PP, PE, Nylon 6 and cellulose) presented by DE VRIES [23], yet are smaller by 3%.

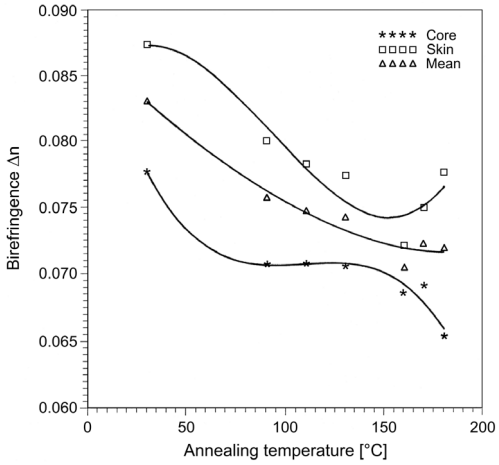

Fig. 7. Variations of Δn_s, Δn_c, and Δn_a with the different annealing temperatures for the constant annealing time of 6 hrs.

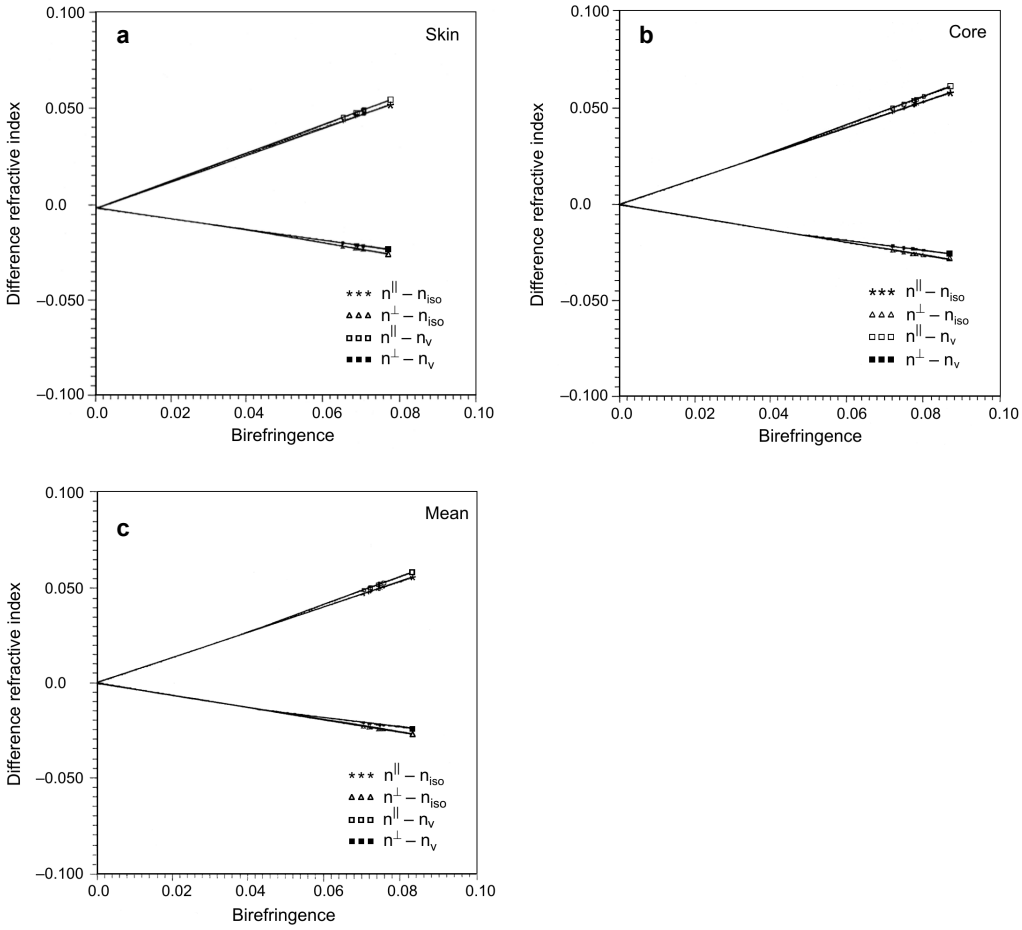

Fig. 8. Variations of Δn_s, Δn_c, Δn_a the refractive index differences $n_s^{\|} - n_{\mathrm{iso}}$, $n_s^{\perp} - n_{\mathrm{iso}}$, $n_s^{\|} - n_v$, $n_s^{\perp} - n_v$ (**a**) $n_c^{\|} - n_{\mathrm{iso}}$, $n_c^{\perp} - n_{\mathrm{iso}}$, $n_c^{\|} - n_v$, $n_c^{\perp} - n_v$ (**b**) $n_a^{\|} - n_{\mathrm{iso}}$, $n_a^{\perp} - n_{\mathrm{iso}}$, $n_a^{\|} - n_v$ $n_a^{\perp} - n_v$ (**c**) at different annealing temperatures for the constant annealing time of 6 hrs.

The apparent volume fraction of crystallinity χ was calculated from Eq. (9) using the calculated density values. Also the calculated values of the mean square density fluctuation $\langle \eta^2 \rangle$, the form birefringence Δn_f, the optical configuration parameter $\Delta\alpha$, the thermal stress σ, the molar refractivity R and the surface reflectivity R' were also calculated at different annealing temperatures. The resultant data are given in Tab 2.

Table 3 contains the calculated values of the number of molecules per unit volume N_2, the mean polarizability of monomer unit of parallel, perpendicular and its mean value, ($\alpha^{\|}$, $\alpha^{\perp}$, and $\bar{\alpha}$) and specific refractivity of the isotropic dielectric of parallel, perpendicular and its mean value ($\varepsilon^{\|}$, $\varepsilon^{\perp}$, and $\bar{\varepsilon}$), at different annealing temperatures and constant time of 6 hrs, for Nylon 66 fibers.

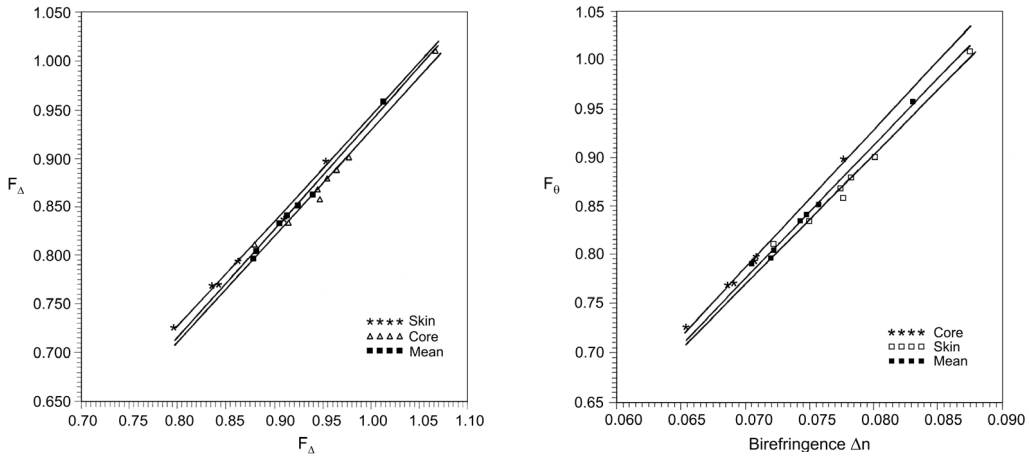

▲

Fig. 9. Relation between corrected values of optical orientation function $F_{\theta(s)}$, $F_{\theta(c)}$, $F_{\theta(a)}$ and the Hermans function $F_{\Delta(s)}$, $F_{\Delta(c)}$, $F_{\Delta(a)}$, at different annealing temperatures for the constant annealing time of 6 hrs.

Fig. 10. Relation between $F_{\theta(s)}$, $F_{\theta(c)}$, $F_{\theta(a)}$ and birfringence Δn_s, Δn_c, Δn_a at different annealing temperature for the constant annealing time of 6 hrs.

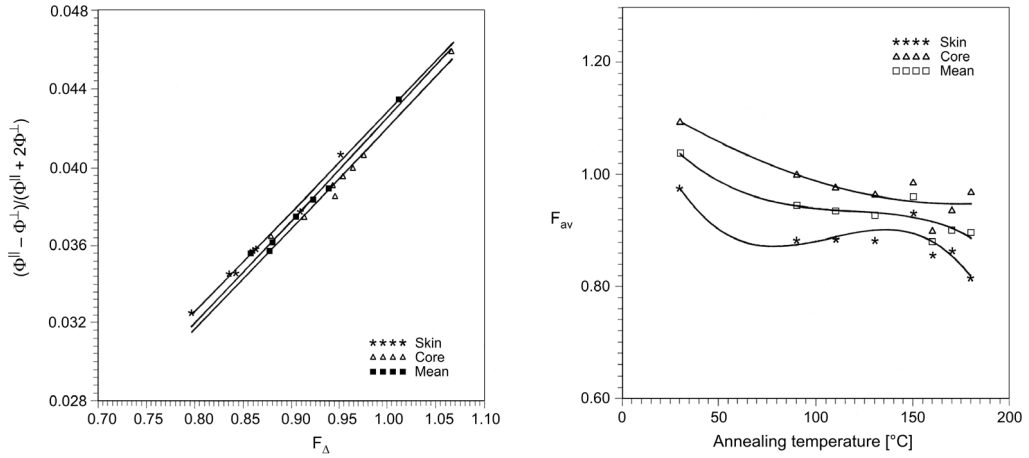

▲

Fig. 11. Relation between Hermans function $F_{\Delta(s)}$, $F_{\Delta(c)}$, $F_{\Delta(a)}$, and $\left|\frac{\Phi^{\parallel}-\Phi^{\perp}}{\Phi^{\parallel}+2\Phi^{\perp}}\right|_{(s)}$, $\left|\frac{\Phi^{\parallel}-\Phi^{\perp}}{\Phi^{\parallel}+2\Phi^{\perp}}\right|_{(c)}$, $\left|\frac{\Phi^{\parallel}-\Phi^{\perp}}{\Phi^{\parallel}+2\Phi^{\perp}}\right|_{(a)}$ at different annealing temperatures for the constant annealing time of 6 hrs.

Fig. 12. Relation between the average orientation F_{av} of fiber at different annealing temperatures for the constant annealing time equal to 6 hrs.

Figure 9 shows the relation between corrected values of optical orientation function $F_{\theta(s)}$, $F_{\theta(c)}$, $F_{\theta(a)}$, and the Hermans function $F_{\Delta(s)}$, $F_{\Delta(c)}$, $F_{\Delta(a)}$, for different annealing temperature with constant annealing time 6 hrs.

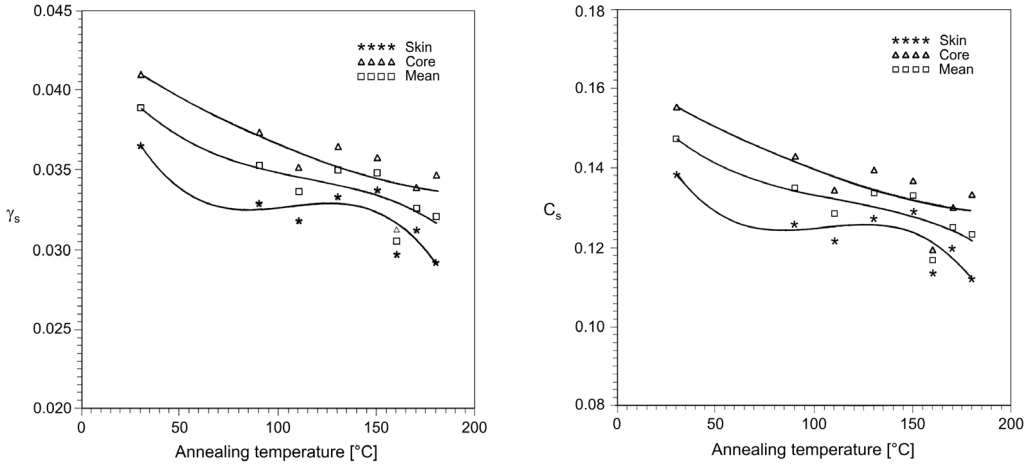

▲

Fig. 13. Relation between the segment anisotropy γ_s of fiber at different annealing temperatures for the constant annealing time equal to 6 hrs.

Fig. 14. Relation between the stress optical coefficient C_s of fiber at different annealing temperatures for the constant annealing time of 6 hrs.

Figure 10 shows the relation between the birefringence Δn_s, Δn_c, Δn_a and the optical orientation function $F_{\theta(s)}$, $F_{\theta(c)}$, $F_{\theta(a)}$ for fibers characterized by different annealing temperatures.

Figure 11 shows the relation between Hermans function $F_{\Delta(s)}$, $F_{\Delta(c)}$, $F_{\Delta(a)}$ and $\left|\frac{\Phi^{\parallel}-\Phi^{\perp}}{\Phi^{\parallel}+2\Phi^{\perp}}\right|_{(s)}$, $\left|\frac{\Phi^{\parallel}-\Phi^{\perp}}{\Phi^{\parallel}+2\Phi^{\perp}}\right|_{(c)}$, $\left|\frac{\Phi^{\parallel}-\Phi^{\perp}}{\Phi^{\parallel}+2\Phi^{\perp}}\right|_{(a)}$ for different annealing temperatures, which give the linear relation and from that we find the value of $\frac{\Delta\alpha}{3\alpha_o}$, which is equal to 0.05. The same occurs for the skin and core layers because this constant is related to the structure constituents.

The average orientation F_{av} was calculated from Eq. (14) and was plotted against the annealing temperatures as shown in Fig. 12. In addition, the segment anisotropy γ_s and the stress optical coefficient C_s, were also calculated and plotted against annealing temperatures in Figs. 13 and 14. The parameters γ_s and C_s decrease with increasing annealing temperatures.

4. Discussion

The structure of man-made fibers is often differentiated radially through their cross-section. The natural source of such a differentiation is provided by solidification processes (heat, crystallization, *etc*.). Therefore, different properties of skin and core may be the result of crystalline texture morphology and other factors.

From the previous data and the corresponding figures obtained in this work several remarks can be made.

The variation in $n_s^{\parallel}$, $n_c^{\parallel}$, $n_a^{\parallel}$ as well as in $P_s^{\parallel}$, $P_c^{\parallel}$, $P_a^{\parallel}$ and during the thermal treatment, is greater than in $n_s^{\perp}$, $n_c^{\perp}$, $n_a^{\perp}$, $P_s^{\perp}$, $P_c^{\perp}$ and $P_a^{\perp}$, although the general trend is almost similar. This indicates that the reorientation of Nylon 66 fibers is stronger in the parallel direction than in the perpendicular one, *i.e.*, Δn_s, Δn_c and Δn_a as well as ΔP_s, ΔP_c and ΔP_a are positive.

At the constant annealing time equal to 6 hrs, at the temperature increasing from 90 to 180 °C, the behaviour of the layers' mean refractive indices, birefringence, polarizabilities and isotropic refractive indices is approximately exponential.

A general deduction from the figures of the present work is that the fiber was affected by isothermal annealing keeping $n_c < n_a < n_s$ for both the parallel and perpendicular fiber axes.

Synthetic polymer fibers play an important role in the textile industry, where most textiles are now mixed with synthetic yarns. Therefore, investigation of the characteristic properties of these fibers aids in the main end use. The degree of orientation, crystallinity and other structural parameters are correlated to the final fiber use. So, the degree of orientation could vary significantly from one fiber to another, depending on the fiber history during manufacturing and subsequent processing operations.

Just as birefringence yields information about the crystallinity and orientation of polymer molecular chains, the isotropic refractive index of medium gives not only information about the molecular package but also specification of the unit cell of crystalline part.

So, in order to explain different variations in our results, it was essential to take the following assumptions into account:

– All thermally structural variations may be considered irreversible, at temperatures higher than the glass transition temperature;

– The most compact non-crystalline structure is not essentially the ordered structure or, in the other words, the oriented macromolecular structure may not be the most compact non-crystalline structure. When a polymeric fiber is annealed, its structural behaviour is changed due to accumulation of several structural processes, which are responses for both annealing temperature and time [42]–[46].

5. Conclusions

From the above discussion and considerations the following conclusions can be drawn:

– Multiple-beam Fizeau fringes method showed that the fiber surface (skin) has a different annealing effect than its core. The microinterferograms are clear to identify these differences in optical path variations. The results may be used for monitoring the isothermal process of these polymer fibers.

– Measurements of the refractive indices indicated that the structure of the fiber along its axis is different from that across its axis, which is expectedly due to the anisotropic phenomena for these fibers.

– The annealing process affects other physical properties (swelling, dyability, electrical, dielectric, colour, mechanical, *etc*.) which needs further studies to detect which properties are improved by the annealing of Nylon 66 fibers.

– As there are variations in the density due to the change in isotropic refractive index n_{iso} also the crystallinity and crystalline parameters of the fiber material varied systematically with different annealing conditions.

– There are visual colour changes of Nylon 66 fibers due to different annealing conditions in air (*i.e*., due to the presence of oxygen).

– It is clear that the multiple-beam Fizeau fringes (and the acoustic methods) are useful and quick techniques to clarify the mechanism of the optical and density parameters of Nylon 66 fibers in different thermal conditions.

– It is clear that $a = 0.5$ (Eq. (6) constant) is constant whatever physical process affects the fiber.

– Calculating the degree of crystallinity and the total birefringence leads to calculation of the form birefringence (Tab. 2), which must not be neglected to explain structural phases in some fibers.

– Following the continuous changes occurring during variations caused by annealing process, we can monitor the changes induced, due to thermal treatments to obtain the same material with new physical properties.

– The value of calculated "form birefringence" in Tab. 2 increases or decreases for Nylon 66 according to the ratio between crystalline and amorphous regions, depending on the annealing conditions.

– Comparison between n_{iso} and n_v (Tab. 1) shows that every equation has its own merit. In the case where the density of material under investigation is known, n_{iso} is more accurate, being indicative of mass redistribution due to any physical changes.

– The molar refractivity changes and the segment anisotropy decreases as the thermal annealing time changes.

– The surface reflectivity R' increases as times of annealing increase.

– The thermal stress σ is nearly constant at different annealing times and constant temperature, Tab. 2.

We conclude from the above results and considerations that the practical importance of these measurements is that they provide acceptable results for the opto-thermal parameters. Since change of $n_s^{\parallel}$, $n_s^{\perp}$, $n_c^{\parallel}$, $n_c^{\perp}$, $n_a^{\parallel}$, $n_a^{\perp}$, *etc*. is a consequence of the material heat treatment, so reorientation of Nylon 66 fiber may occur not only during manufacturing but also due to the annealing process. It can also be admitted that multiple-beam technique is very promising to reveal the changes due to the annealing process for the optical behaviour of skin-core structure of Nylon 66 fibers.

References

[1] KORNYUKHINA T.A., KOCHERVUSKÜ V. V., ZELENEV YU.V., Polym. Sci. **20** (1979), 803.
[2] STATTON W.O.S., J. Polym. Sci. **A-210** (1972), 1587.
[3] DECONDIA F., VITTORIA V., J. Polym. Sci. Phys. Ed. **23** (1985), 1217.
[4] WILLIAM G., PERKINS P., PORTER S.R., J. Mater. Sci. **2** (1977), 2355.

[5] ZACHARIODES A.Z., PORTER S.R., *The Strength and Stiffness of Polymers*, Marcel Dekker, New York, Basel 1983, p. 121.
[6] HAWARD W., STARKWEATHER J.R., GEARGE E.M., HANSAN J.E., RODER T.M., BROOKS R.E., J. Polym. Sci. **1** (1956), 201.
[7] WYCOFF H., J. Polym. Sci. **62** (1962), 82.
[8] FOUDA I.M., EL-TONSY M.M., SHABAN A.M., J. Mater. Sci. **26** (1991), 5085.
[9] HAMZA A.A., FOUDA I.M., EL-TONSY M.M., EL-SHARKAWY F.M., J. Appl. Polym. Sci. **56** (1995), 1355.
[10] FOUDA I.M., SEISA E.A., EL-FARAHATY K.A., Polymer Testing **15** (1996), 3.
[11] SIMMENS S.C., J. Textile Inst. (Trans.) **46** (1955), 715.
[12] MOREHEAD F.F., SISSON W.A., Textile Res. J. **15** (1945), 443.
[13] BARAKAT N., HINDELEH A.M., Text. Res. J. **34** (1964), 581.
[14] FAUST R.C., Proc. R. Soc. Lond. B **65** (1952), 48.
[15] HAMZA A.A., FOUDA I.M., SOKKAR T.Z.N., EL-BAKARY M.A., Polym. Int. **39** (1996), 129.
[16] HAMZA A.A., EL-TONSY M.M., FOUDA I.M., EL-SAID A.M., J. Appl. Polym. Sci. **57** (1995), 265.
[17] FOUDA I.M., SEISA E.A., J. Polym. & Polymer Composites, **4** (1996), 247.
[18] *Ibidem* p. 489.
[19] FOUDA I.M., EL-NICKLAWY M.M., NASER E.M., EL-AGAMY R.M., J. Appl. Polym. Sci. **60** (1996), 1247.
[20] EL-NICKLAWY M.M., FOUDA I.M., J. Text. Inst. **71** (1980a), 252.
[21] BARAKAT N., EL-HENNAWI H.A., Text. Res. J. **41** (1971), 391.
[22] MILLS N.J., [Ch. 7, P. 492, in A. D. Jenkins, *Polymer Science: A Materials Science Handbook*, Vol. 1 Ch. 7, North Holand Pub. Co. Amsterdam- London 1972, p. 492.
[23] DE VRIES H., Z Kolloid, Polym. Sci. **257** (1979), 226.
[24] FOUDA I.M., KABEEL M.A., EL-SHARKAWY F.M., J. Polymer & Polymer Comosites **5** (1997), 431.
[25] HERMANS P.H., PLATZEK P., Kolloid-Z. **88** (1939), 233.
[26] KRATKY O., Kolloid-Z. **64** (1933), 213.
[27] WARD I.M., J. Polym. Sci. Polym. Sym. **58** (1977), 1.
[28] HERMANS P.H., *Contributions to the Physics of Cellulose Fibers*, North Holland, Amsterdam 1946.
[29] CUNNINGHAM A., WARD I.M., WILLIS H.A., ZICHY V., Polymer **15** (1974), 749.
[30] FOUDA I.M., KABEEL M.A., EL-SHARKAWY F.M., J. Polymer & Polymer Composites **5** (1997), 203.
[31] LE BOURVELLEE G., BEAUTEMPS J., J. Appl. Polym. Sci. **39** (1990), 329.
[32] BRONDRUP J., IMMERGUT E.H., *Polymer Handbook*, 2nd Ed., John Wiley, 1975, p. 779.
[33] JENKINS A.D., *Polymer Science: A Materials Science Handbook*, Vol. 1, North Holand, Amsterdam–London 1972, Ch. 7, p. 496.
[34] HAPPY F., *Applied Fiber Science*, Vol. 1, Academic Press, London 1983, p. 130.
[35] FISCHER E.W., FAKIROW S., J. Mater. Sci. **11** (1976), 1041.
[36] WESOLOWSKA E., LEWASKIEWICZ W., J. Polym. Sci. Phys. Ed. **26** (1988), 2573 [in ref. MURTHY N.S., BRAY R.G., CARREALE S.T., MOORE R.A.F., Polymer **36** (1995), 3863].
[37] RIANDE E., GUZMAN J., J. Polym. Sci. Phys. Ed. **22** (1984), 917.
[38] JENKINS A.D., *Materials Science Handbook, Polymer Science*, Vol. 1, North-Holland, Amsterdam 1972, Ch. 7, p. 505.
[39] HEMSLEY D.A., *Applied Polymer Light Microscopy*, Elsevied Press, London 1964, p. 88.
[40] FOUDA I.M., KABEEL M.A., EL-SHARKAWY F.M., J. Polymer & Polymer Composites **7** (1997), 355.
[41] WARD I.M., *Structure and Properties of Oriented Polymer*, Applied Science Publishers, London 1975, p. 57.
[42] SARKISYAN V.A., ASRATYAN M.G., MKHITORYAN A.A., KATRDZHYAN K.KH., DADIVANYAN A.K., Vysokomal. Sayed **A 27** (1985), 1331.

[43] SAMELUS J.R., *Structural Polymer Properties*, Vol. 20, John Wiley, New York 1974, pp. 50–60.
[44] POLUKHIN P., GORELIK S., VORTONTSOV V., *Physical Principles of Plastic Deformation*, Mir, Moscow 1983, p. 275.
[45] BASSETT D.C., *Principles of Polymer Morphology*, Cambridge University Press, Cambridge 1981, p. 124
[46] WILLIAMS D.J., *Polymer Science and Engineering*, Prentice-Hall, New Jersey 1971, p. 188.

Received December 23, 2002